# Single-shot layered reflectance separation using a polarized light field camera

Jaewon Kim[†,§]     Shahram Izadi[‡]     Abhijeet Ghosh[†]

[†]Imperial College London
[‡]Microsoft Research (Redmond)
[§]Korea Institute of Science and Technology (KIST)



(a) Two-way polarized light field (TPLF) camera     (b) Camera raw     (c) Spec. + single scatt.     (d) Diffuse (depolarized)

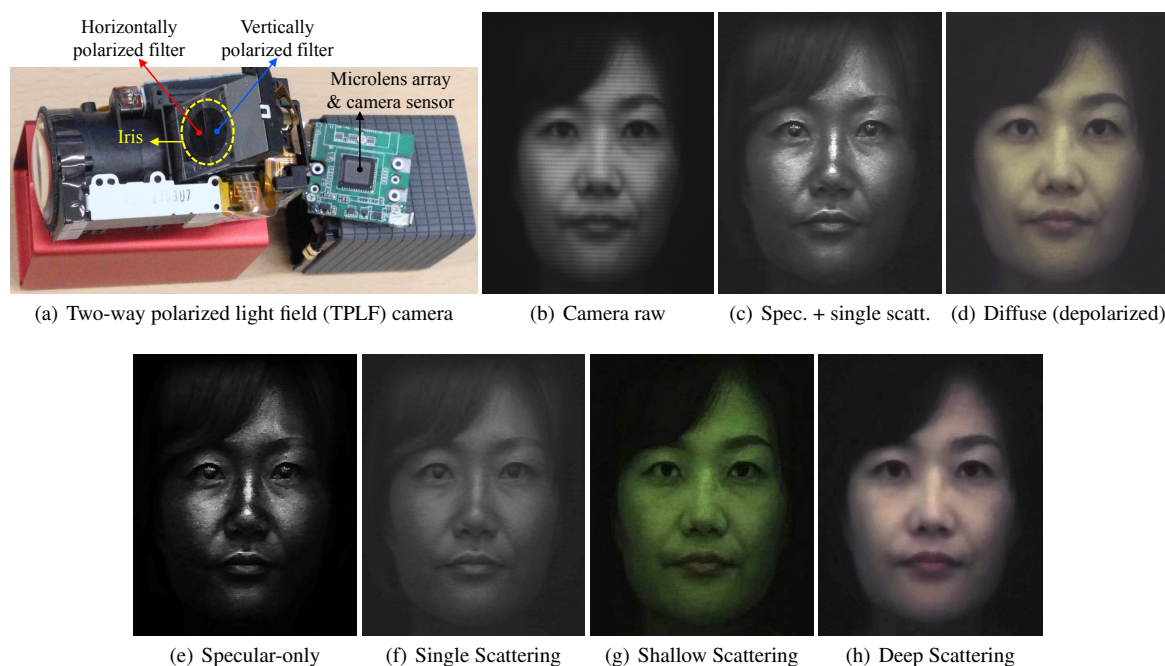(e) Specular-only     (f) Single Scattering     (g) Shallow Scattering     (h) Deep Scattering

Figure 1: Single shot layered reflectance separation using proposed two-way polarized light field (TPLF) camera. (a) Components of the TPLF camera in disassembly. (b) A raw photograph taken by the TPLF camera under uniform (hemi-spherical) illumination (circular microlens pixels visible in zoomed-in view). (c, d) Standard polarization preserving (specular + single scatter) and depolarized (diffuse) reflectance components separated with light field sampling. (e, f) Specular-only and single scattering further separated from the polarization preserving component (c). (g, h) Shallow and deep scattering components further separated from diffuse component (d). Note (e) through (h) present results of layered reflectance separation comparable to the multi-shot technique of Ghosh et al. [GHP*08].

## Abstract

*We present a novel computational photography technique for single shot separation of diffuse/specular reflectance as well as novel angular domain separation of layered reflectance. Our solution consists of a two-way polarized light field (TPLF) camera which simultaneously captures two orthogonal states of polarization. A single photograph of a subject acquired with the TPLF camera under polarized illumination then enables standard separation of diffuse (depolarizing) and polarization preserving specular reflectance using light field sampling. We further demonstrate that the acquired data also enables novel angular separation of layered reflectance including separation of specular reflectance and single scattering in the polarization preserving component, and separation of shallow scattering from deep scattering in the depolarizing component. We apply our approach for efficient acquisition of facial reflectance including diffuse and specular normal maps, and novel separation of photometric normals into layered reflectance normals for layered facial renderings. We demonstrate our proposed single shot layered reflectance separation to be comparable to an existing multi-shot technique that relies on structured lighting while achieving separation results under a variety of illumination conditions.*

## 1. Introduction

Realistic reproduction of appearance of an object or a subject has been a long-standing goal in computer graphics. With advances in digital photography over the last couple of decades, measurement based appearance modeling has become very popular for various realistic rendering applications. This is particularly true for realistic appearance modeling of human faces, which has signficiant applications in the entertainment sector (e.g., games and film visual effects). Thus, several techniques and measurement setups have been developed over the years for acquisition of material and facial reflectance [DRS08, WLL*09]. However, it is quite common in practice for the measured reflectance data to be fit to appropriate analytic or physically based reflectance models for usage in a rendering system. This practice of fitting measurements to appropriate models has motivated separation of measurements into individual reflectance components, such as specular (surface) and diffuse (subsurface), as an important initial step in measurement based appearance modeling. Researchers have thus investigated various techniques for separation of individual reflectance components, particularly for dielectric materials, including color based and polarization based separation techniques [NFB97, MZKB05, DHT*00].

Given the high quality of separation achieved with polarization imaging, polarization based separation has emerged as the preferred solution for high end facial capture applications [ARL*10]. However, this has traditionally resulted in a multi-shot technique for reflectance acquisition with polarization (to capture both the parallel and cross polarized states), or required complicated acquisition setups (e.g., multiple cameras sharing an optical axis through a beam-splitter) to simultaneously image various polarization states. Further fine-grained separation of layered reflectance (e.g, in skin) has been even more challenging and has, thus far, required a sophisticated multi-shot approach combining polarization imaging and computational illumination [GHP*08].

In this paper, we propose a novel technique for efficient aquisition of surface and subsurface reflectance using a two-way polarized light field (TPLF) camera along with novel computational analysis of the acquired light field data for layered reflectance separation. Besides standard diffuse-specular separation, our approach achieves single-shot acquisition (under uniform polarized illumination) of layered reflectance albedos spanning specular, single scattering, shallow scattering and deep scattering (see Figure 1). Besides albedo estimation, the technique can also be coupled with polarized spherical gradient illumination to acquire photometric diffuse and specular normal maps and can further enable novel layered separation of photometric normals for realistic rendering applications.

To summarize, the specific technical contributions of this work are as follows:

- Practical realization of two-way polarized light field imaging by attaching orthogonal linear polarizers to the pupil plane of the main lens of a commercial light field camera. This allows simultaneous acquisition of two orthogonal polarization states of incoming rays in a single shot and enables separation of diffuse and specular reflectance using angular light field sampling.

- Novel analysis of the acquired light field data for layered reflectance separation in the angular domain. This enables estimation of layered reflectance albedos using single shot capture under uniform illumination, and novel layered separation of photometric normals using polarized spherical gradient illumination.

The rest of the paper is organized as follows: we first review some related work in Section 2 before presenting our proposed TPLF camera and its application for single shot diffuse-specular separation in Section 3. Section 4 then presents our novel computational light field analysis for layered separation of facial reflectance including albedo and photometric normals. We finally present some rendering applications of separated facial reflectance and additional examples and analysis of our technique in Section 5.

## 2. Related work

We first present a brief review of relevant previous work on reflectance separation, facial reflectance capture and light field imaging.

### 2.1. Reflectance separation

Separation of acquired reflectance into individual diffuse and specular components has long been of interest for various computer graphics and vision applications such as reflectometry and photometric stereo. In dielectric materials, specular reflectance corresponds to first surface reflection while diffuse reflectance corresponds to subsurface reflection and is responsible for the characteristic color of a material. This is why researchers have investigated color based methods for reflectance separation [Sha92]. Nayar et al. [NFB97] proposed combining color space analysis with polarization imaging for separation of specular and diffuse reflectance on textured objects where pure color based methods are not very successful. Mallick et al. [MZKB05] instead exploit a color space transform to remove the specular component for a photometric stero application. The method works for dichromatic materials but does not provide an estimate of the diffuse color. Debevec et al. [DHT*00] proposed employing polarized illumination in conjunction with polarization imaging to separate specular and diffuse reflectance in faces lit by a point light source and fit the separated data to a microfacet BRDF model. Nayar et al. [NKGR06] have proposed a computational illumination technique for separating direct and indirect (global) light transport in a scene using phase shifted high frequency structured lighting. Lamond et al. [LPGD09] proposed a related method for reflectance separation using high frequency angular phase shifting of environmental illumination. More recently, Tunwattanapong et al. [TFG*13] have proposed illuminating an object with (higher order) spherical harmonic illumination for reflectance separation/estimation. Similarly, Aittala et al. [AWL13] have proposed illuminating a planar sample with Fourier basis functions for frequency domain separation of diffuse and specular reflectance. However, these approaches require a static scene due to reliance on multi shot computational illumination for reflectance separation. In contrast, our proposed approach requires only single shot acquisition under a fixed lighting condition and hence could be easily applied for dynamic scenes

as well. Ghosh et al. [GCP*10] have proposed reflectometry under circularly polarized spherical illumination by imaging the complete Stokes parameters of reflected polarization. Similarly, specular highlights can be removed by accurately estimating the polarization angle of the specular highlight using measurements of linear Stokes parameters [FJYY15]. However, these approaches require multi-shot acquisition and a specialized filter wheel to rotate appropriate polarizers in front of the camera to acquire the Stokes parameters. Instead, we employ two fixed orthogonal linear polarizers in the optical path of a light field camera for single shot polarization based reflectance separation.

## 2.2. Facial reflectance capture

Debevec et al. [DHT*00] proposed acquiring a 4D reflectance field of a face using a light stage for image based relighting applications. While producing photorealistic facial renderings, the approach requires a large set of photographs (150-200) for recording a view-dependent reflectance field. Weyrich et al. [WMP*06] employed a similar light stage apparatus to densely record facial reflectance using a combination of multiview capture (16 views) and dense sampling of the incident illumination (150 directions). They employed a combination of multiview analysis and intensity based separation of diffuse and specular reflectance observed over the facial surface and fit the acquired data to appropriate surface reflectance (for specular) and subsurface scattering (for diffuse) models for facial renderings. While such dense sampling of reflectance results in high quality facial renderings from any viewpoint, it is also less practical due the requirement of acquiring and processing a large amount of data for rendering.

More recently, Ma et al. [MHP*07] proposed a novel photometric stereo technique based on spherical gradient illumination that requies only four spherical lighting conditions (using an LED sphere) and provides high quality estimates of facial albedo and surface normals. They further proposed employing polarized spherical illumination and polarization difference imaging on the camera to separate acquired facial reflectance into specular and diffuse albedos and normals maps which is shown to produce high quality facial renderings with hybrid normal rendering. Ghosh et al. [GHP*08] further built upon the capture setup of Ma et al. and proposed a practical method for acquiring layered facial reflectance with a limited number of observations. They used a combination of polarized spherical gradient illumination and polarized frontal point source illumination for separation and fitting of specular reflectance and single scattering in the polarization preserving component. Furthermore, Ghosh et al. separated shallow and deep scattering using a combination of cross-polarization (to discard specular reflectance) and direct-indirect separation [NKGR06] using structured lighting patterns. While both Ma and Ghosh et al.'s approaches drastically reduce data acquisition compared to traditional light stage based facial capture techniques, they are still multi-shot techniques requiring extended capture of several seconds with a DSLR camera: Ma's method requires eight shots to capture the spherical gradients in both polarization states, while Ghosh et al.'s method further adds six additional photographs under frontal projector illumination for layered facial reflectance acquisition. Ghosh's method also requires additional processing to associate reflectance parameters acquired

under different illumination conditions for rendering. In contrast, our proposed approach is able to separate layered reflectance albedos acquired under uniform polarized illumination in just a *single* photograph. And the approach can be coupled with polarized spherical gradient illumination to enable novel layered separation of photometric normals using just three additional photographs. Donner et al. [DWd*08] have also proposed multispectral imaging under flash illumination coupled with inverse rendering to estimate spectral scattering properties of skin for layered skin renderings. However, the method is limited to measurements of a small skin patch and cannot be easily scaled to full facial measurement.

Facial capture with polarized spherical gradient illumination was originally restricted to a single viewpoint due to the employed view dependent linear polarization pattern [MHP*07]. Spherical gradient illumination has also been employed for facial performance capture by Fyffe et al. [FHW*11], who employed unpolarized illumination to enable multiview capture and proposed a heurisitics based separation of facial reflectance for rendering purposes. Subsequently, Ghosh et al. [GFT*11] have extended polarized spherical gradient illumination for multiview face capture by proposing two orthogonal linear polarization patterns (latitude-longitude) on the LED sphere that are symmetric about the vertical axis. This allows multiview capture with a static vertical linear polarizer on the camera. However, their approach still requires multi-shot acquisition to acquire both states of polarization and also requires a sophisticated lighting setup with the ability to switch the polarization state of illumination. Researchers have also proposed alternate passive facial capture techniques [BBB*10, BHPS10] under uniform illumination that achieve impressive results of facial geometry reconstruction. However, these passive approaches do not separate facial reflectance and instead employ the flatly lit facial photograph as the diffuse albedo for rendering. Recently, Fyffe & Debevec [FD15] have proposed a single shot method for estimating diffuse and specular albedos and a surface normal map using polarized color gradient illumination. They employ a coaxially aligned camera pair (with a polarizing beam splitter) to simultaneously capture mutually perpendicular polarization states and employ the latitude-longitude polarization patterns [GFT*11] to simultaneously emit two orthogonal polarization states. Furthermore, they encode the X, Y, and Z spherical gradients with RGB color gradient illumination which is simultaneously emitted from the polarized LED sphere. While achieving single shot acquisition of separated albedo and normal maps (modulo slightly lower quality of reflectance data), the approach requires an extremely sophisticated lighting setup with a polarized RGB LED sphere and multiple carefully calibrated cameras. In contrast, we propose a simple modification of an off-the-shelf light field camera that enables single shot reflectance separation under various common illumination setups.

## 2.3. Light field and multimodal imaging

Practical light field capture has been widely explored to acquire 2D spatial + 2D angular coordinates of incoming rays within a single camera housing using a microlens array [NLB*05] or a patterned mask [VRA*07] design. Such 4D ray information has been previously utilized for various applications including generation of sythetically refocused images [NLB*05], reducing glare effects
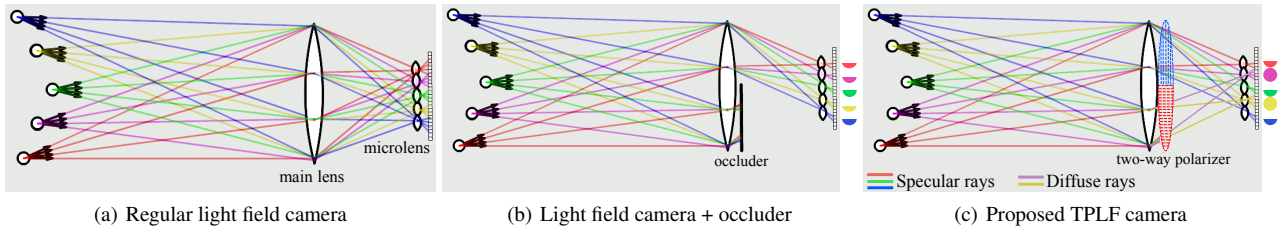
Figure 2: Ray simulation[†] for illustrating the concept of proposed TPLF camera. (a) Regular light field imaging with a camera with a microlens array for diffuse and specular rays. If a half occluder is placed behind the main lens as in (b), only half the rays reach the sensor. Our TPLF camera in (c) has the occluder replaced with a two-way polarizer which is half vertically and half horizontally polarized.

in camera lenses [RAWV08], and separation of direct and scattered rays through a participating media [KLMR10]. Narasimhan et al. [NN02] presented a design to capture multidimensional information including dynamic range and spectral information through a specialized Bayer pattern. The approach also tries to increase effective spatial resolution of the imaging system by exploiting local correlations in the imaged functions through a learned model based on training data. Also related to our work, researchers have investigated light field capture based on a pinhole array [HEAL09], and mirror reflections [MRK*13] respectively in conjunction with optical filters in the entrance pupil of a main lens. These designs modulate the acquired 4D light field with various optical filters to image multidimensional information such as dynamic range, multiple spectrum or polarization but require calibrated laboratory setups including optical tables for precise alignment of various components. Closer to our approach, recently a single light field photograph was used to remove specularities by exploiting point-consistency between angular samples of a scene point [TSW*15]. The point-consistency is preserved in principle for diffuse pixels and not for specular pixels, so its measurement can directly distinguish both reflections. However, the method only works for the edge of specular region since in practice point-consistency is also preserved for the saturated pixels (bright central parts) of a specular region. While the above methods share a similar conceptual approach, ours is a much more practical realization consisting of a simple modification of a compact off-the-shelf light field camera. We also propose a novel application of layered reflectance separation which has not been previously explored with light field imaging.

## 3. Two-way polarized light field imaging

We now describe our acquisition technique for diffuse and specular reflectance based on our novel two-way polarized light field (TPLF) camera which addresses the challenge of capturing two different polarization states in a single shot. Figure 2 (a) shows a ray diagram for a regular light field camera. For simplicity, let us assume there are five scene points emitting four rays in diffuse or specular reflection. The four rays emitted from each point in various directions are focused into a point by the main lens and dispersed into sensor pixels by the microlens array. Let us think about a half occluder placed

---

† Based on Andrew Adams's optical bench toolkit http://graphics.stanford.edu/~abadams/lenstoy.swf

at the back of the main lens as shown in Figure 2 (b). Only half of the rays reach the camera sensor and the other half are blocked by the occluder resulting in the semicircular rays as shown on the right. In the case of our TPLF camera shown in Figure 2 (c), the occluder is replaced with a two-way linear polarizer, where the upper half is vertically polarized and bottom half is horizontally polarized. This way, the blocked and unblocked rays in the occluder case now pass through the horizontal and the vertical polarizers respectively. If the scene is illuminated with vertically polarized light, specular reflection rays (illustrated in red, green, and blue) can pass through only the vertically polarized region. This results in the semicircular images via the microlens array on the right side. On the other hand, diffuse reflection rays (illustrated in purple and yellow) can pass through the entire polarizer (due to depolarization) and result in the fully circular images on the right. Consequently, given linearly polarized illumination, our TPLF camera provides a semicircular and a fully circular microlens image for specular and diffuse surface reflections respectively. These respective microlens imaging regions are predetermined once using a calibration photograph and TPLF photographs can thereafter be automatically processed using this calibration information. Note that pixels in a raw photograph are sensed through a mosaic color filter. Hence, we have to additionally demosaic color pixels by averaging color information in 4×4 pixel regions to generate a color TPLF photograph.

Figure 1 (a) shows the actual TPLF camera used for our experiments, which was built from a Lytro Red Hot 16GB camera to which we attached a two-way linear polarizer in the pupil plane of the main lens. The camera produces a light field image at 1080×1080 resolution with a 331×381 microlens array. Although Lytro software and some other methods allow increasing the resolution of light field images to higher than the number of microlenses, we only carry out single-pixel generation per each microlens image for simplicity which means our processed images have 331×381 resolution.

### 3.1. Diffuse-specular separation

Figure 3 (a) shows an example photograph captured by the TPLF camera of a plastic mannequin. In the inset image of the eye, each circular pattern corresponds to the contribution of rays passing through each microlens. It can be seen that the lower semi-circular region has very bright intensity which is contributed by strong polarization preserving specular rays imaged through a microlens. As

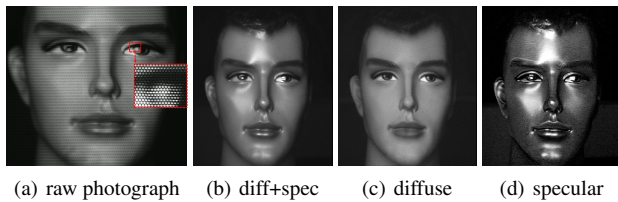(a) raw photograph  (b) diff+spec  (c) diffuse  (d) specular

Figure 3: (a) A raw photograph of a mannequin taken with our TPLF camera. (b) Parallel polarized (diffuse + specular) component, and separated (c) diffuse, and (d) specular component images generated from the raw. The mannequin is made of glossy plastic.
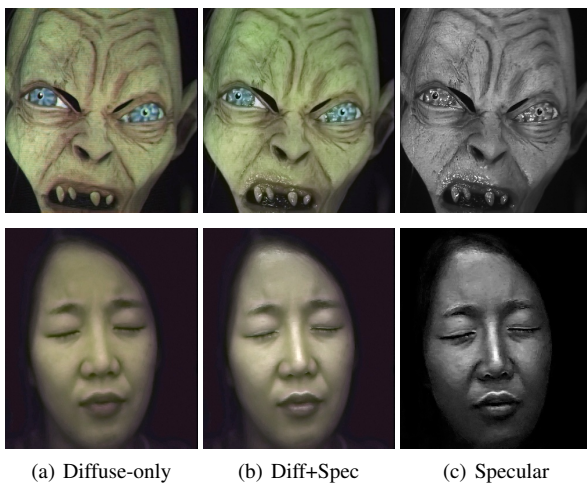


(a) Diffuse-only  (b) Diff+Spec  (c) Specular

Figure 4: Diffuse-only, diffuse+specular, and specular component images generated from a single TPLF camera photograph for a maquette (top row) and a subject's face (bottom row). The Gollum maquette is made of a compound of silicon and rubber.

indicated in our ray simulation (Figure 2, c), the upper semicircular region has a lower intensity since the specular rays are filtered out by cross-polarization in this region. Conversely, diffuse rays which are depolarized contribute equally to the whole circular microlens image. By exploiting this spatial separation between diffuse and specular rays, parallel polarized (diffuse+specular) and cross-polarized diffuse-only images could be generated from sampling pixels over each respective semicircular region. Here, the diffuse+specular component image (Figure 3, b) was generated by averaging pixels sampled from lower semicircular regions. Likewise, a diffuse-only component image (Figure 3, c) was generated by averaging pixels from the upper semicircular region. Subtraction of the diffuse-only image from the diffuse+specular image generated the specular (polarization preserving) component image as shown in Figure 3, (d). Note that due to cross-polarization, the diffuse-only component (c) is imaged with only half intensity.

Figure 4 presents additional examples of separated diffuse-only, diffuse+specular, and specular component images for a Gollum maquette and a subject's face, which were generated from a single-shot photograph taken with the TPLF camera. Note that the highly



Figure 5: LED hemisphere for illuminating a subject with polarized spherical illumination.



(a) Diff. albedo  (b) Spec. albedo
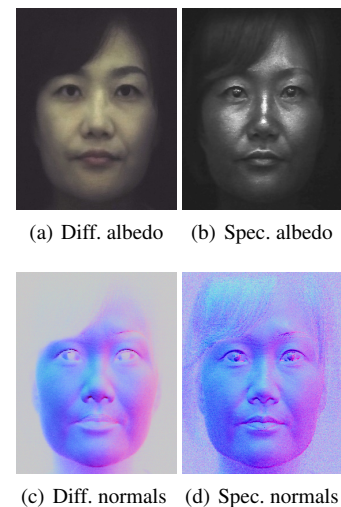
(c) Diff. normals  (d) Spec. normals

Figure 6: Separated diffuse (a, c) and specular (b, d) albedo and photometric normals of a female subject acquired using four measurements under polarized spherical gradient illumination.

specular components in Gollum's eyes and mouth as well as the woman's nose, forehead, and mouth in the diffuse+specular images are completely removed in the diffuse-only images while they are preserved in the specular component images.

The diffuse-specular separation examples shown in Figures 3 and 4, as well the separation result of the female subject shown in Figure 1 were acquired under uniform illumination using an LED hemisphere shown in Figure 5. The hemispherical illumination system consists of a total of 130 LED (5W) light sources. A linear polarizer is mounted in front of each light source and adjustable to rotate along the tangent direction to the light source. We pre-calibrate the polarizer orientation on all the lights to cross-polarize with respect to a frontal camera viewing direction similar to the procedure described in [MHP*07].

Besides recording the reflectance of a subject under constant uniform illumination to estimate the albedo, the LED hemisphere also allows us to record the subject's reflectance under polarized spherical gradient illumination in order to estimate photometric normals.

Figure 6 shows separated diffuse and specular normals estimated for the female subject shown in Figure 1 using three additional measurements under the X, Y and Z spherical gradients. As can be seen, the diffuse normal is smooth due to blurring of surface detail due to subsurface scattering while the specular normal contains high frequency skin mesostructure detail due to first surface reflection [MHP*07]. However, we only need to make a total of four measurements for separated albedo and photometric normals as we do not need to flip a polarizer in front of the camera [MHP*07] or switch polarization on the LED sphere [GFT*11] in order to observe two orthogonal polarization states.

## 4. Layered reflectance separation

The previous section described diffuse-specular separation using respective sampling of cross- and parallel-polarized semi-circular regions of a microlens in our TPLF camera. In this section, we now describe a novel computational method to obtain layered reflectance separation from a single-shot photograph using angular light field sampling. It should be noted that in skin the specular component separated with polarization difference imaging is actually also mixed with some single scattering which also preserves polarization [GHP*08]. This corresponds to the "specular" values of each microlens image in our TPLF camera photograph as shown in Figure 7, (b) which are obtained after difference imaging of the lower and upper semi-circular regions of the microlens and include contributions of specular reflectance and single scattering. Similarly, the diffuse values in the upper semi-circular region of the microlens include contributions of both shallow and deep subsurface scattering. We make the observation that our TPLF camera allows us to angularly sample these various reflectance functions in a single photograph. As depicted in Figure 7 (a), these reflectance functions have increasingly wider reflection lobes ordered as follows: specular reflectance has a sharper lobe than single scattering in the polarization preserving component, and both shallow and deep scattering have wider reflectance lobes as they are the result of multiple subsurface scattering. Among these, deep scattering has a wider lobe than shallow scattering due to a greater number of subsurface scattering events.

Now, the circularly arranged pixels of the microlens angularly sample these reflectance functions as follows: the brighter pixels within each semi-circular region sample both narrow and wide reflectance lobes while the darker pixels sample only the wider reflectance lobes which have lower peaks. This motivates us to propose an angular sampling method to separate these various layered reflectance components. We first rely on the observation that specular rays are much brighter than single scattered rays in skin. Hence, we propose separation of these two components by separately sampling high and low intensity values in the polarization preserving component. Each semi-circular region inside a microlens observes a total of $9 \times 4 = 36$ values. We sort these observed values according to their brightness and employ a threshold for the separation. We emperically found averaging the brightest 30% values as specular reflection and averaging the remaining (darker) 70% values as the single scattering component gave good results in practice (see Figure 1 e, f).

Next, we assume that deep scattering has a wider angular lobe than
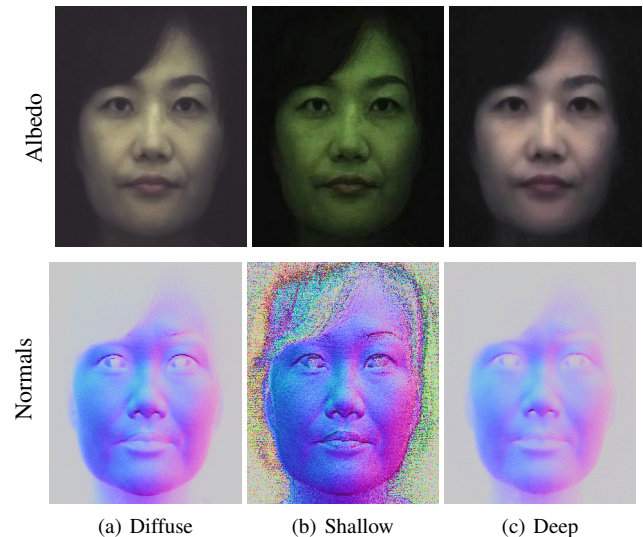


(a) Diffuse      (b) Shallow      (c) Deep

Figure 8: Comparison of albedos and normal maps for diffuse component, and separated shallow and deep scattering.

shallow scattering in the diffuse component since it scatters further out spatially. Hence, we model deep and shallow scattering components in the diffuse-only region of a microlens image as shown in Figure 7, (b): darker (outer) pixels correspond to only deep scattering while brighter (inner) pixels contain both shallow and deep scattering. This modeling assumes that the lobe of shallow scattering is narrow enough not to contribute to the entire diffuse-only region of the microlens. We sample pixels in the darker outer region of each microlens image and average them for generating a deep scattering image as shown in Figure 1 (h). Subtracting the deep scattering value from shallow+deep scattering pixels in the brighter inner region generated the shallow scattering image in Figure 1 (g). We empirically found that using the sampling ratio of darkest 40% values for estimating deep scattering and the brightest 60% values for estimating shallow+deep provided qualitatively similar results of separation compared to those reported by Ghosh et al. [GHP*08], with similar color tones and scattering amount in each component. Finally, in order to employ the separated shallow and deep scattering components as albedos for layered rendering, we need one additional step of radiometric calibration to ensure that the sum of the two separated shallow and deep albedos matches the total diffuse reflectance albedo in order to ensure that the separation is additive similar to the separation of [GHP*08].

Note that our assumptions about the width of the reflectance lobes is supported by the modeling of Ghosh et al. [GHP*08] where they applied the multipole diffusion model [DJ05] for shallow scattering and the dipole diffusion model [JMLH01] for deep scattering to approximately model epidermal and dermal scattering. They measured scattering profiles with projected circular dot patterns and fitted the measurements to these diffusion models. While the outer two third region of each projected pattern was fitted accurately with the deep scattering model, the inner one-third region was not because of the additional shallow scattering component. Differences in lobe widths of shallow and deep scattering is also supported
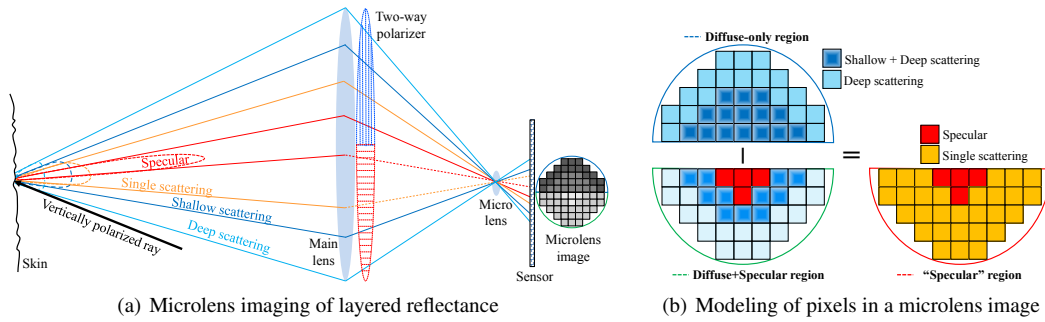
(a) Microlens imaging of layered reflectance  (b) Modeling of pixels in a microlens image

Figure 7: *Angular sampling process of the TPLF camera for layered reflectance. (a) Ray diagram through a two-way polarizer and a microlens. (b) Modeling of pixel allocation in a microlens image.*
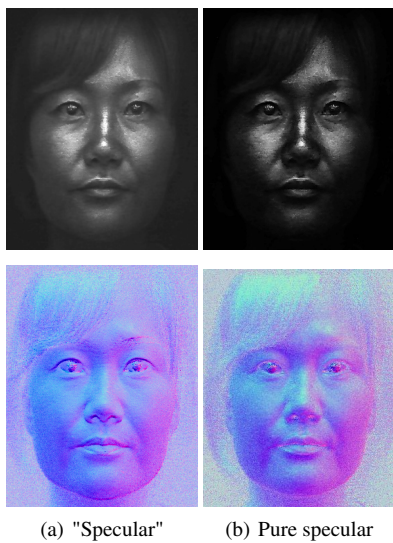


(a) "Specular"  (b) Pure specular

Figure 9: *Removal of single scattering from specular reflectance in the polarization preserving component (a) for novel computation of pure specular albedo and photometric normals (b). Top-row: specular albedo. Bottom-row: specular normals.*

by Henyey-Greenstein phase function [HK93] where the forward scattering parameter g is (0.90, 0.87, 0.85) and (0.85, 0.81, 0.77) for epidermal and dermal layers respectively in (R, G, B) [Jac13]. Since the smaller parameter values make the lobe wider, deep scattering occurring at a dermal layer is assumed to have a wider lobe. Also, considering the modeled layer thicknesses for epidermal (0.001-0.25mm) and dermal layers (1-4 mm) in the literature, the radiative transport equation implies that the thicker layer makes the scattering lobe wider [NN03].

Besides separating layered reflectance albedos under uniform polarized illumination, we go further than previous work to further separate diffuse normals into shallow and deep scattering normal maps (Figure 8) by applying our novel angular domain light field sampling to polarized spherical gradient illumination. As can be seen, the shallow scattering normals contain more surface detail than the regular diffuse normals estimated with spherical gradi-

ents, while the deep scattering normals are softer and more blurred than the corresponding diffuse normals. We believe this novel layered separation of photometric normals in addition to albedo separation can be very useful for real time rendering of layered skin reflectance with a hybrid normal rendering approach. Figure 9 demonstrates another similar separation where we remove single scattering from the polarization preserving component to estimate pure specular albedo, and for the first time, a pure specular normal map (b). Note that specular normal maps have been used to estimate accurate high frequency skin mesostructre detail for high-end facial capture [MHP*07, GFT*11]. However, "specular" normals (a) as acquired by Ma and Ghosh et al. have some single scattering mixed with the signal which acts as a small blur kernel on the specular surface detail and can also slightly bend the true orientation of the specular normal. Removal of this single scattering from the data used to compute pure specular normals has the potential for further increasing the accuracy and resolution of facial geometry reconstruction.

## 5. Applications and analysis

We now present rendering applications of standard diffuse-specular and layered reflectance separation using our TPLF camera. Figure 10, (a) presents hybrid normal rendering for a female subject (lit by a point light source) according to the method proposed by Ma et al. [MHP*07]. Here, the diffuse and specular albedo and normal maps were acquired using four photographs with the TPLF camera under polarized spherical gradient illumination using the LED hemisphere. As can be seen, the specular reflectance highlights the skin surface mesostructure while the diffuse reflectance has a soft translucent appearance due to blurring of the diffuse normals due to subsurface scattering. Note that the facial geometry for the hybrid normal rendering was acquired separately using multiview stereo with additional DSLR cameras (see Figure 5). Figure 10, (b) presents a novel layered hybrid normal rendering where the diffuse albedo and normals have been further separated into shallow and deep scattering albedo and normals respectively. Note that due to the additive property of the separation, the result of layered rendering (b) is very similar to the standard hybrid normal rendering (a) in this case.

Figure 11 presents a few editing applications of the proposed lay-
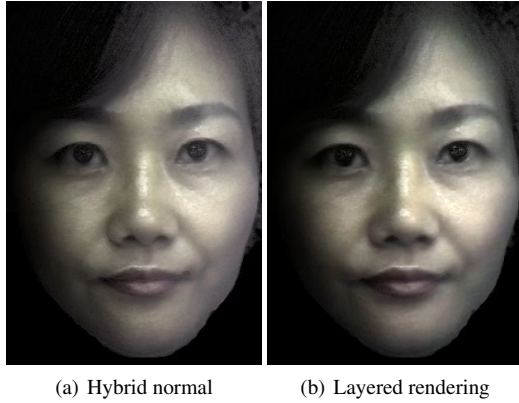
(a) Hybrid normal          (b) Layered rendering

Figure 10: *Hybrid normal renderings with data acquired using four photographs under polarized spherical gradient illumination. (a) Rendering with separate diffuse and specular normals as proposed by Ma et al. [MHP\*07]. (b) Layered hybrid normal rendering with diffuse reflectance further separated into shallow and deep albedo and normals.*

ered hybrid normal rendering with separated shallow and deep scattering albedo and normals. Here, we have removed the specular layer from the rendering to highlight the edits to the diffuse layer. The top row presents results of diffuse rendering with the regular diffuse albedo shaded with the shallow scattering normal in (a), and deep scattering normal in (b) respectively. As can be seen, the skin appearance is dry and rougher when shaded with shallow scattering normal, and softer and more translucent when shaded with the deep scattering normal compared to the regular hybrid normal rendering (Figure 10, a). The bottom row presents results of layered hybrid normal rendering where we have edited the shallow and deep scattering albedos to enhance one component relative to the other. As can be seen, enhancing the shallow scattering albedo (w.r.t. deep) (c) makes the skin appearance more pale and dry, while enhancing the deep scattering albedo (w.r.t. shallow) (d) makes the skin more pink in tone and softer in appearance. The availability of layered reflectance albedos and normals with our TPLF acquisition approach makes such appearance editing operations easily possible.

Figure 12 presents results of shallow and deep scattering separation obtained with various intensity thresholds for light field sampling and compares these single-shot separation results with that obtained using the computational illumination technique of Ghosh et al. [GHP\*08] (Figure 12, d) which uses cross-polarized phase shifted high frequency structured lighting patterns. As can be seen, our shallow and deep scattering albedo separation with single-shot TPLF imaging achieves similar qualitative results of layered separation compared to the multi-shot technique of [GHP\*08]. Here, we found the intensity threshold of 60%:40% (brighter 60% values used to estimate shallow+deep, darker 40% used to estimate deep) for the separation of shallow and deep scattering to have the most qualitiative similarity to structured lighting based separation. Note that the multi-shot result was somewhat degraded in comparison to the original paper. This is due to subtle subject motion ar-
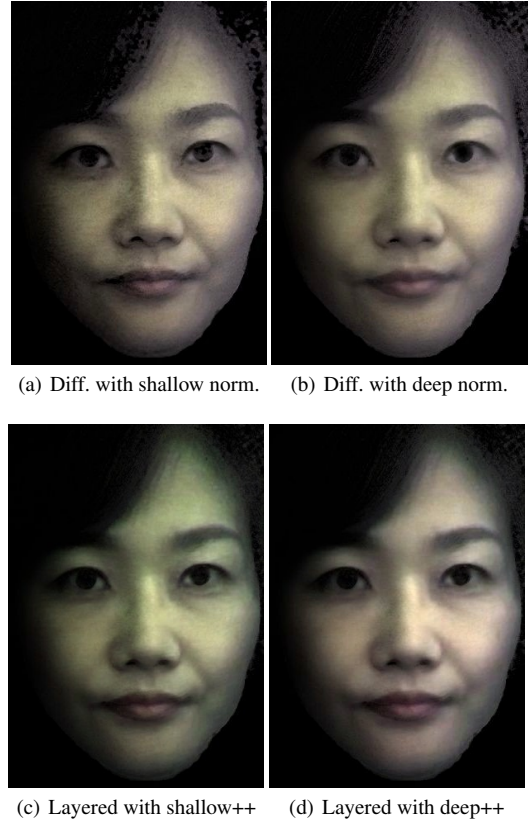


(a) Diff. with shallow norm.          (b) Diff. with deep norm.



(c) Layered with shallow++          (d) Layered with deep++

Figure 11: *Editing applications of layered reflectance and normals. Top-row: Diffuse rendering using shallow scattering normal (a), and deep scattering normal (b) respectively for shading the diffuse albedo. Bottom-row: Layered hybrid normal rendering with relative enhancement of the shallow scattering albedo (c), and relative enhancement of the deep scattering albedo (d) respectively.*

tifacts during the 4 shots required to acquire the response to phase shifted stripes. We employed a commodity Canon EOS 650D camera with sequential triggering to acquire the 4 shots while Ghosh et al. [GHP\*08] used a special head stabilization rig and fast capture with burst mode photography (using a high end Canon 1D Mark III camera) to prevent such motion artifacts. This further highlights the advantage of our proposed single-shot method.

One advantage of our method is that we employ uniform spherical illumination for separation which is more suitable for albedo estimation than frontal projector illumination required for structured lighting. The projector illumination also impacts subject comfort during acquisition: the subject had to keep very still and their eyes closed during acquisition of the structured lighting patterns for the separation. We, however, note that there are some visible color differences between the results of separation with the TPLF camera and separation with structured lighting. These color differences can be mainly attributed to differences in color temperatures of the two respective illumination systems (LED hemisphere vs projector), as well as differences in respective camera color response curves

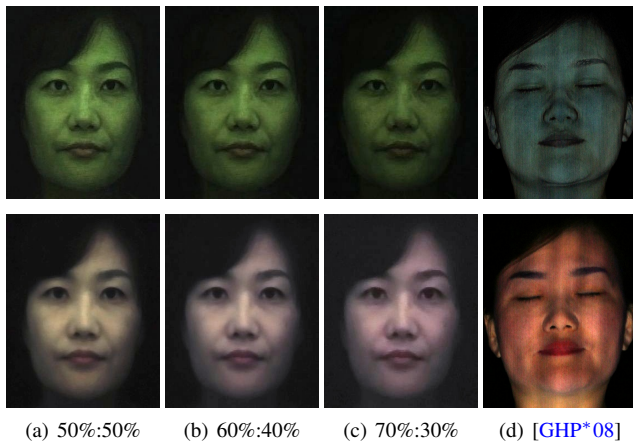(a) 50%:50%    (b) 60%:40%    (c) 70%:30%    (d) [GHP*08]

Figure 12: Comparison of shallow and deep separation with single-shot TPLF imaging and the multi-shot technique of Ghosh et al. [GHP*08]. (a – c) Different split ratios of intensity averaging (brighter (shallow+deep)% : darker (deep)%) with TPLF imaging. (d) Separation with phase shifted structured lighting patterns.



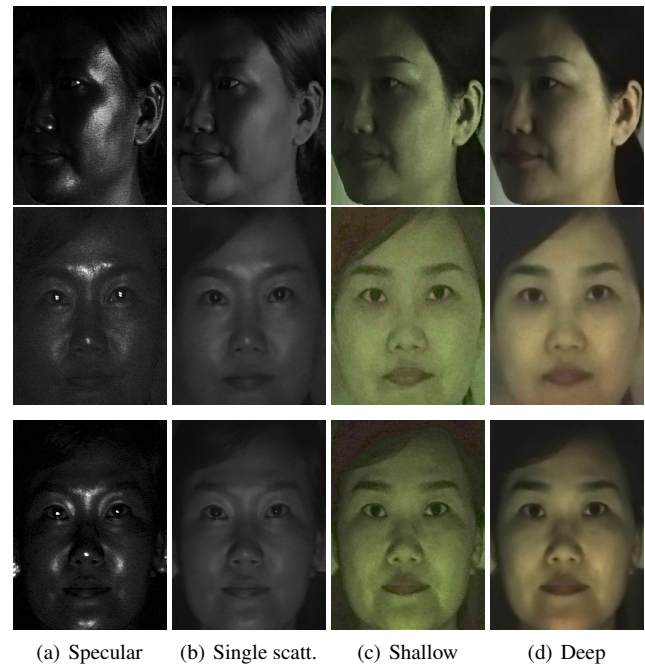(a) Specular    (b) Single scatt.    (c) Shallow    (d) Deep

Figure 13: Layered reflectance separation with single-shot TPLF imaging under various illumination conditions. Top-row: uniform LCD panel illumination. Center-row: Four point lights. Bottom-row: Single point light.

(the data for structured light based separation was acquired using a Canon DSRL camera). The color reproduction with the Lytro camera is not as vivid because it is based on our own implementation of demosaicing which may not be optimal.

Finally, we analyze the quality of layered reflectance separation with TPLF imaging under various other illumination setups that are commonly available. Figure 13 presents results of single-shot layered reflectance separation on a subject's face lit from the side with uniform illumination from a 32" desktop LCD panel (top row), a set of four point light sources (with two on each side) approximating a typical photometric stereo setup (center row), and finally lit with only a single point light source from the front (bottom row). Here, we simply used smartphone LED flashes as the point light sources in our experiment. Note that the LCD panel already emits (vertical) linearly polarized illumination so we did not need to explicitly polarize it for the measurement. We mounted plastic linear polarizer sheets (vertically oriented) in front of the phone LED flashes for the other measurements. Among these, employing uniform illumination emitted by the LCD panel resulted in the highest quality of separation, particularly for shallow and deep scattering. Such an illumination setup could also be used in conjunction with passive facial capture systems such as that employed by Bradley et al. [BHPS10]. Furthermore, our method also achieves good qualitative layered reflectance separation under just a set of point light sources (and even with a single point light) which has not been previously demonstrated. We believe this can be very useful for appearance capture with commodity facial capture setups. We however note that the separation results with the point light sources suffer from poorer signal-to-noise ratio due to the larger dynamic range between the specular highlight and the diffuse reflectance compared to when using spherical or extended (LCD) illumination.

### 5.1. Limitations and discussion

Since our TPLF photography is based on light field imaging, it suffers from the classical issue of resolution trade-off with a light field camera. However, the good news is that light field camera resolution is rapidly increasing, e.g., the Lytro Illum now has 2K spatial resolution. The Lytro camera does not provide an official way to manipulate the raw light field photograph, so we implemented our own microlens sampling and color demosaicing pipeline. This clearly leads to sub-optimal results as we could not obtain precise information on microlens position for precise pixel sampling and also colors are not reproduced as vividly as desirable. The color reproduction can be improved by measuring a color chart with the TPLF camera and transforming measured color values to sRGB color space. Our separation assumes that the incident illumination is polarized with its axis either vertically or horizontally oriented in order to match the orientation of our two-way polarizer. Fortunately, this is not very hard to achieve in practice with many illumination setups. The TPLF camera also has a restricted dynamic range compared to DSLR cameras which is why it is currently more suitable for acquisition with spherical or extended illumination compared to point light sources. However, we expect this dynamic range issue to be resolved with improvements in light field camera technology.

We currently emperically set the intentisty thresholds for layered reflectance separation. Further research would be required to relate such separation thresholds to physiological characteristics of reflec-

tion and scattering of light in various layers of skin. We also simply render skin appearance with hybrid normal rendering approach using the separated reflectance albedos and photometric normals. However, many rendering systems instead implement full blown subsurface scattering simulations to achieve translucency effects. Besides scattering albedos, such a rendering approach requires an estimate of translucency (diffuse mean free path) which we do not currently measure. However, the approach of Zhu et al. [ZGP*13] could be employed with our data to estimate per pixel translucency from four measurements under polarized spherical gradient illumination. Furthermore, our separation of diffuse albedo and normals into shallow and deep scattering albedo and normals might enable estimation of layered translucency parameters for rendering shallow and deep scattering using such an approach. Our imaging approach for layered reflectance separation may also have applications in other domains such as cosmetics where the technique could be applied to separate a cosmetic layer from the underlying skin reflectance or applications in industrial or cultural heritage sectors for separation of layered materials such as paints or pigments.

## 6. Conclusion

To summarize, we propose a novel computational photography method for single-shot separation of diffuse and specular reflectance as well as more fine grained separation of layered reflectance using a two-way polarized light field camera. Our imaging approach allows estimation of diffuse, specular, single scattering, shallow scattering, and deep scattering albedos from a single photograph captured under uniform polarized illumination. We further demonstrate novel layered separation of photometric normals acquired using polarized spherical gradient illumination with just three additional photographs. Thus, our approach significantly reduces the number of required measurements for layered reflectance acquisition compared to existing multi-shot techniques while enabling novel appearance editing applications with layered reflectance and normal maps. We also demonstrate our single-shot reflectance separation technique to work well in practice with a variety of commodity illumination setups. This can be very useful for appearance acquisition with commodity facial capture setups that employ passive imaging. Our method could be extended in the future to estimate more complete reflectance information such as parameters to describe a full BRDF or a BSSRDF with a combination of appropriate light field filtering and controlled illumination. And the proposed layered reflectance separation approach could have applications in various other domains such as dermatology/cosmetics, automotive or cultural heritage applications.

## 7. Acknowledgements

## References

[ARL*10]  ALEXANDER O., ROGERS M., LAMBETH W., CHIANG J.-Y., MA W.-C., WANG C.-C., DEBEVEC P.: The digital emily project: Achieving a photorealistic digital actor. *Computer Graphics and Applications, IEEE 30*, 4 (2010), 20–31. 2

[AWL13]  AITTALA M., WEYRICH T., LEHTINEN J.: Practical SVBRDF capture in the frequency domain. *ACM Trans. Graph. 32*, 4 (July 2013), 110:1–110:12. 2

[BBB*10]  BEELER T., BICKEL B., BEARDSLEY P., SUMNER B., GROSS M.: High-quality single-shot capture of facial geometry. *ACM Trans. on Graphics (Proc. SIGGRAPH) 29*, 3 (2010), 40:1–40:9. 3

[BHPS10]  BRADLEY D., HEIDRICH W., POPA T., SHEFFER A.: High resolution passive facial performance capture. *ACM Transactions on Graphics (TOG) 29*, 4 (2010), 41. 3, 9

[DHT*00]  DEBEVEC P., HAWKINS T., TCHOU C., DUIKER H.-P., SAROKIN W., SAGAR M.: Acquiring the reflectance field of a human face. In *Proceedings of the 27th annual conference on Computer graphics and interactive techniques* (2000), ACM Press/Addison-Wesley Publishing Co., pp. 145–156. 2, 3

[DJ05]  DONNER C., JENSEN H. W.: Light diffusion in multi-layered translucent materials. *ACM Trans. Graph. 24*, 3 (2005), 1032–1039. 6

[DRS08]  DORSEY J., RUSHMEIER H., SILLION F.: *Digital Modeling of Material Appearance*. Morgan Kaufmann Publishers Inc., San Francisco, CA, USA, 2008. 2

[DWd*08]  DONNER C., WEYRICH T., D'EON E., RAMAMOORTHI R., RUSINKIEWICZ S.: A layered, heterogeneous reflectance model for acquiring and rendering human skin. *ACM Trans. Graph. 27*, 5 (Dec. 2008), 140:1–140:12. 3

[FD15]  FYFFE G., DEBEVEC P.: Single-shot reflectance measurement from polarized color gradient illumination. In *International Conference on Computational Photography* (2015). 3

[FHW*11]  FYFFE G., HAWKINS T., WATTS C., MA W.-C., DEBEVEC P.: Comprehensive facial performance capture. *Computer Graphics Forum (Proc. Eurographics) 30*, 2 (2011). 3

[FJYY15]  FANG L., JIANDONG T., YANDONG T., YAN W.: An image highlights removal method with polarization principle. *In Proceedings of ICMMITA* (2015), 402–407. 3

[GCP*10]  GHOSH A., CHEN T., PEERS P., WILSON C. A., DEBEVEC P.: Circularly polarized spherical illumination reflectometry. In *ACM Transactions on Graphics (TOG)* (2010), vol. 29, ACM, p. 162. 3

[GFT*11]  GHOSH A., FYFFE G., TUNWATTANAPONG B., BUSCH J., YU X., DEBEVEC P.: Multiview face capture using polarized spherical gradient illumination. *ACM Transactions on Graphics (TOG) 30*, 6 (2011), 129. 3, 6, 7

[GHP*08]  GHOSH A., HAWKINS T., PEERS P., FREDERIKSEN S., DEBEVEC P.: Practical modeling and acquisition of layered facial reflectance. *ACM Trans. Graph. 27*, 5 (Dec. 2008), 139:1–139:10. 1, 2, 3, 6, 8, 9

[HEAL09]  HORSTMEYER R., EULISS G., ATHALE R., LEVOY M.: Flexible multimodal camera using a light field architecture. *International Conference on Computational Photography* (2009). 4

[HK93]  HANRAHAN P., KRUEGER W.: Reflection from layered surfaces due to subsurface scattering. *In Proceedings of ACM SIGGRAPH* (1993), 165–174. 7

[Jac13]  JACQUES S. L.: Optical properties of biological tissues: a review. *Med. Biol. 58* (2013), R37–61. 7

[JMLH01]  JENSEN H. W., MARSCHNER S. R., LEVOY M., HANRAHAN P.: A practical model for subsurface light transport. *In Proceedings of ACM SIGGRAPH* (2001), 511–518. 6

[KLMR10]  KIM J., LANMAN D., MUKAIGAWA Y., RASKAR R.: Descattering transmission via angular filtering. *ECCV 2010 LNCS 6311* (2010), 86–99. 4

[LPGD09] LAMOND B., PEERS P., GHOSH A., DEBEVEC P.: Image-based separation of diffuse and specular reflections using environmental structured illumination. In *IEEE International Conference on Computational Photography (ICCP)* (2009). 2

[MHP*07] MA W.-C., HAWKINS T., PEERS P., CHABERT C.-F., WEISS M., DEBEVEC P.: Rapid acquisition of specular and diffuse normal maps from polarized spherical gradient illumination. In *Proceedings of the 18th Eurographics Conference on Rendering Techniques* (2007), EGSR'07, Eurographics Association, pp. 183–194. 3, 5, 6, 7, 8

[MRK*13] MANAKOV A., RESTREPO J. F., KLEHM O., HEGEDÜS R., EISEMANN E., SEIDEL H.-P., IHRKE I.: A reconfigurable camera add-on for high dynamic range, multi-spectral, polarization, and light-field imaging. *ACM Trans. Graph. (Proc. SIGGRAPH 2013) 32*, 4 (July 2013), 47:1–47:14. 4

[MZKB05] MALLICK S. P., ZICKLER T. E., KRIEGMAN D., BELHUMEUR P. N.: Beyond lambert: Reconstructing specular surfaces using color. In *Computer Vision and Pattern Recognition, CVPR, IEEE Computer Society Conference on* (2005), vol. 2, Ieee, pp. 619–626. 2

[NFB97] NAYAR S. K., FANG X.-S., BOULT T.: Separation of reflection components using color and polarization. *Int. J. Comput. Vision 21*, 3 (Feb. 1997), 163–186. 2

[NKGR06] NAYAR S., KRICHNAN G., GROSSBERG M., RASKAR R.: Fast separation of direct and global components of a scene using high frequency illumination. *ACM Transactions on Graphics 25*, 3 (2006), 935–943. 2, 3

[NLB*05] NG R., LEVOY M., BRDIF M., DUVAL G., HOROWITZ M., HANRAHAN P.: Light field photography with a hand-held plenoptic camera. *Stanford Tech Report* (2005). 3

[NN02] NAYAR S. K., NARASIMHAN S. G.: Assorted pixels : Multi-sampled imaging with structural models. In *ECCV* (June 2002). 4

[NN03] NARASIMHAN S., NAYAR S.: Shedding light on the weather. *In Proceedings of IEEE CVPR* (2003), 665–672. 7

[RAWV08] RASKAR R., AGRAWAL A., WILSON C. A., VEERARAGHAVAN A.: Glare aware photography: 4d ray sampling for reducing glare effects of camera lenses. *ACM Trans. Graph. 27*, 3 (2008), 1–10. 4

[Sha92] SHAFER S. A.: Color. Jones and Bartlett Publishers, Inc., USA, 1992, ch. Using Color to Separate Reflection Components, pp. 43–51. URL: http://dl.acm.org/citation.cfm?id=136809.136817. 2

[TFG*13] TUNWATTANAPONG B., FYFFE G., GRAHAM P., BUSCH J., YU X., GHOSH A., DEBEVEC P.: Acquiring reflectance and shape from continuous spherical harmonic illumination. *ACM Transactions on Graphics (TOG) 32*, 4 (2013), 109. 2

[TSW*15] TAO M., SU J.-C., WANG T.-C., MALIK J., RAMAMOORTHI R.: Depth estimation and specular removal for glossy surfaces using point and line consistency with light-field cameras. *IEEE TPAMI* (2015), 1–14. 4

[VRA*07] VEERARAGHAVAN A., RASKAR R., AGRAWAL A., MOHAN A., TUMBLIN J.: Dappled photography: Mask enhanced cameras for heterodyned light fields and coded aperture refocusing. *ACM Trans. Graph. 26*, 3 (July 2007). 3

[WLL*09] WEYRICH T., LAWRENCE J., LENSCH H. P. A., RUSINKIEWICZ S., ZICKLER T.: Principles of appearance acquisition and representation. *Found. Trends. Comput. Graph. Vis. 4*, 2 (Feb. 2009), 75–191. 2

[WMP*06] WEYRICH T., MATUSIK W., PFISTER H., BICKEL B., DONNER C., TU C., MCANDLESS J., LEE J., NGAN A., JENSEN H. W., GROSS M.: Analysis of human faces using a measurement-based skin reflectance model. *ACM Trans. Graph. 25*, 3 (July 2006), 1013–1024. 3

[ZGP*13] ZHU Y., GARIGIPATI P., PEERS P., DEBEVEC P., GHOSH A.: Estimating diffusion parameters from polarized spherical-gradient illumination. *IEEE Computer Graphics and Applications 33*, 3 (2013), 34–43. 10